Design guidelines for granular particles in a conical centrifugal filter

A.F.M. Bizard[a], D.D. Symons[a,*], N.A. Fleck[a], G.C. Grimwood[b]

[a] *Cambridge University Engineering Department, Trumpington Street, Cambridge, CB2 1PZ, UK*

[b] *Thomas Broadbent and Sons Ltd., Queen Street South, Huddersfield, HD1 3EA, UK*

Abstract

Essential design criteria for successful drying of granular particles in a conical continuous centrifugal filter are developed in a dimensionless fashion. Four criteria are considered: minimum flow thickness (to ensure sliding bulk flow rather than particulate flow), desaturation position, output dryness and basket failure. The criteria are based on idealised physical models of the machine operation and are written explicitly as functions of the basket size l_{out}, spin velocity Ω and input flow rate of powder Q_p. The separation of sucrose crystals from liquid molasses is taken as a case study and the successful regime of potential operating points (l_{out}, Ω) is plotted for a wide range of selected values of flow rate Q_p. Analytical expressions are given for minimum and maximum values of the three independent parameters (l_{out}, Ω, Q_p) as a function of the slurry and basket properties. The viable operating regime for a conical centrifugal filter is thereby obtained as a function of the slurry and basket properties.

*Corresponding author. Email: Tel: +44 1223 760502; Fax: +44 1223 332662
Email address: digby.symons@eng.cam.ac.uk (D.D. Symons)
URL: http://www-edc.eng.cam.ac.uk/people/dds11.html (D.D. Symons)

Keywords: design, filtration, centrifugation, powders, separation, drying

Nomenclature

List of Roman symbols

Bo	Bond number
C_i	Dimensionless limit for criteria i
K	Carman-Kozeny permeability empirical constant
M	Liquid mass fraction
N_{cap}	Capillary number
Q	Volumetric flow rate
R	Dimensionless radial position
Ro	Rossby number
S	Relative saturation
X_i	Dimensionless group for criteria i
Z	Ratio of fluid drainage and powder sliding velocities
a	Slip velocity dependency coefficient for wall shear traction
$\tilde{a}$	Dimensionless empirical slip velocity dependency parameter
b	Coefficient of friction for powder against wall
$\hat{b}$	Ratio of the coefficient of friction b to the cone slope $\tan\alpha$
d_p	Average particle size
$\tilde{d}$	Minimum through-thickness number of particles for sliding bulk flow
g	Acceleration due to gravity
g^*	Centripetal acceleration
h	Thickness
k_p	Powder permeability

$\tilde{k}$	Dimensionless empirical coefficient for powder permeability
l_{out}	Basket radius at outlet in cylindrical co-ordinates
$\dot{m}$	Total input mass flow rate of slurry
n_p	Powder porosity
p	Pressure
q	Superficial velocity of liquid through thickness of powder cake
r	Radial position in a spherical co-ordinate system
s	Particle specific area
u	Through thickness averaged radial velocity
v	Local radial velocity
v_{out}	Circumferential velocity at outlet
z	Through-thickness co-ordinate, origin z=0 at the wall

List of Greek symbols

Σ	Design space
Ψ	Particle sphericity
Ω	Cone angular velocity
α	Cone semi-angle
γ	Fluid surface tension
ζ	Safety factor for basket failure
θ	Polar angle
κ	Ratio of permeability of screen and powder
μ_f	Fluid dynamic viscosity
ξ	Dimensionless position of the desaturation point
ρ	Density
$\bar{\rho}$	Ratio of the powder density to that of the fluid
σ	Normal stress
τ	Shear stress
ϕ	Hoop angle

List of subscripts

$_b$	Basket (cone)
$_{bkf}$	Basket failure
$_{conv}$	Fluid convected by powder movement
$_{dry}$	Target dryness condition
$_{eff}$	Effective
$_f$	Fluid
$_i$	Criteria: 1) bulk flow, 2) desaturation, 3) dryness, 4) basket failure
$_{in}$	Inlet
$_{out}$	Outlet
$_p$	Powder or particle
$_{ref}$	Reference value
$_{seep}$	Fluid seepage through powder
$_{tot}$	Total (fluid and solid)
$_y$	Yield (of basket)

1. Introduction

1.1. Centrifugal filters

Centrifugal filters are commonly used in the food processing and chemical industries in order to separate the liquid and solid phases of a mixture. There exist two main types of centrifugal filter: *batch* machines with a cylindrical basket and *continuous* machines with a conical basket. The present study focuses on continuous conical centrifuges, which are most commonly used in the sucrose industry to separate sucrose crystals from molasses. Swindells (1982) and Greig (1995) studied the functioning of these machines in a semi-

empirical fashion. While their work provides valuable insight into the operation of conical centrifuges in the sucrose industry it does not fully address the underlying mechanics. Consequently, only a limited number of operating parameters have been used to optimize the design and operation of the sucrose machine. Application of the results for sucrose to pharmaceutical, chemical or other food products has also proved difficult. This study aims to provide fundamental guidelines for the design of a conical centrifugal filter, based upon idealised physical models of the machine.

1.2. Typical operation of a continuous centrifuge

The operation of a continuous conical centrifuge is now described through the example of a typical sucrose industry machine. The rotating conical basket of the machine, sketched in Fig.1, has a jump in cone angle along its length: a lower impervious cone has a semi-angle of $\alpha = 15^\circ$ whereas the upper perforated cone has a semi-angle of $\alpha = 30^\circ$. The basket is about 1m in diameter at outlet and spins at 1800 RPM to provide a maximum centripetal acceleration of $2000g$. The inside wall of the upper, perforated cone is fitted with a slotted screen, thereby allowing for fluid drainage but preventing powder losses, see Fig.1. The feedstock, in the form of a sucrose/molasses slurry (*massecuite*) of mass moisture fraction M_{in} $\approx$50% and temperature 60°C, is introduced along the spin axis into the lower impervious cone at a constant mass flow rate $\dot{m}$. The slurry acquires the angular velocity of the basket Ω and migrates up the wall of the cone under centrifugal force.[1]

[1]Most of the tangential acceleration occurs in an acceleration cone which deposits the slurry onto the lower impervious cone at an angular velocity already close to Ω.

Sedimentation of the sucrose crystals in the lower impervious cone causes the crystals to tend to settle, and then slide, against the smooth cone wall. Three distinct regions labelled I to III can be identified in the upper perforated cone as indicated in Fig.2a. An idealised microstructure may be assumed to exist in each region, see Fig.2b. In region I the flow is in the over-saturated state: the sucrose crystals have settled into a densely packed layer of height h_p, whereas the excess fluid exists to a height $h_f > h_p$, as shown.[2]

Liquid drainage causes the slurry to evolve into an under-saturated cake of densely packed powder of height h_p in region II. In region II the upper portion of the powder cake is damp and coated with a thin liquid film, while the bottom portion (of height h_f) is still saturated with fluid. Finally in region III, providing the centripetal acceleration is sufficient to overcome capillary forces, the powder is desaturated and only a residual liquid fraction wets the surface of the crystals. The flow in region III consists of a cake of damp powder, of height h_p, sliding over the screen. Region II is therefore the transition zone between flow of over-saturated powder (region I) and flow of damp powder (region III) and is commonly called the *colour line* in the sucrose industry. Further liquid drainage in region III is assumed to be negligible and the damp powder in this region is treated as a homogeneous continuous medium of constant properties.

[2]Here we assume complete initial settlement of the solid phase occurs in the lower impervious cone. In a previous study (Bizard and Symons, 2011) we have compared this assumption with the other extreme of nil settlement at the start of region I. The effect on the downstream regions II and III was found to be negligible.

1.3. Outline of paper

The analysis begins by stating the governing field equations and constitutive law that are assumed to apply in the upper, perforated cone. It is assumed that the feed is a suspension of coarse granular material that settles to an incompressible close packed bed which slips against the cone wall. Essential design criteria are then derived for the successful operation of a conical centrifuge. Restrictions on the input flow rate, outlet circumferential velocity and centripetal acceleration to give successful operation are then obtained from these criteria. Finally, a practical application of this analysis is presented in the form of design maps for the typical case of sucrose massecuite separation.

2. Governing field equations and the constitutive law

Equilibrium, continuity and constitutive relationships for idealised damp granular flow in a spinning cone are now presented. These relationships are then used to define reference values for flow velocity and thickness that are used throughout this paper.

2.1. Equilibrium

A spherical co-ordinate system (r, θ, ϕ) (see Fig.3) is appropriate for describing the flow in a conical centrifugal filter. In most practical situations the flow in the cone is slender: its thickness h is significantly smaller than the radial co-ordinate r. A boundary layer approximation of the momentum equations is therefore applicable. This approach to analysis of flow in a spinning cone has been adopted by Bruin (1969) and Makarytchev et al.

(1997, 1998) for a Newtonian viscous fluid, and by Symons (2011*a*) for a damp powder.

The relative importance of convective, Coriolis and centripetal accelerations in the momentum equations (when written in a rotating frame of reference) may be assessed via the Rossby number Ro as defined by Makarytchev et al. (1997):

$$Ro = \frac{u}{r\Omega \sin\alpha} \approx \frac{\text{convective}}{\text{Coriolis}} \approx \frac{\text{Coriolis}}{\text{centripetal}} \tag{1}$$

where u is the through-thickness averaged radial velocity, Ω the angular velocity of the cone and α is the cone apex angle. In this study we assume that the Rossby number is significantly smaller than unity, so that both convective and Coriolis accelerations are negligible compared to the centripetal acceleration. This assumption is in accordance with observations of typical slender, high viscosity flows observed in industrial conical centrifuges. A consequence of a small Rossby number (i.e. low radial velocity) is that the circumferential slip (in the ϕ-direction) is negligible and therefore the flow has virtually the same angular velocity as the cone at any radius r (see e.g. Symons (2011*a*), Symons (2011*b*)). Analysis is further simplified by assuming that gravity g may be neglected compared to the centripetal acceleration. Given that the three dimensionless groups h/r, Ro and $g/r\Omega^2 \sin\alpha$ are all much less than unity the flow momentum equations may be reduced to the equilibrium statements

$$\frac{\partial p_{tot}}{\partial z} = -\rho g^* \cos\alpha \tag{2}$$

$$\frac{\partial \tau}{\partial z} = -\rho g^* \sin\alpha \tag{3}$$

where p_{tot} and τ are the total normal and shear stresses within the flow (see Fig. 3), z is the through-thickness co-ordinate ($z \approx r(\alpha - \theta)$ where $z \ll r$ and thus $\partial z = -r\partial\theta$), ρ is the local density and

$$g^* = r\Omega^2 \sin\alpha \tag{4}$$

is the centripetal acceleration. At the free-surface of the flow ($z = h$) $p_{tot} = \tau = 0$ and therefore (2-3) reduce to

$$\tau = p_{tot} \tan\alpha \tag{5}$$

throughout the flow thickness at any r.

2.2. Continuity

Assume that the granular particles form an approximately incompressible, densely packed cake with a porosity n_p that is constant throughout the cone. Then, conservation of the volumetric flow rate Q_p of the powder (including voids) dictates that

$$Q_p = 2\pi r u_p h_p \sin\alpha \tag{6}$$

Also, note that Q_p is specified by the total mass flow rate of slurry at inlet $\dot{m}$ via

$$Q_p = \frac{(1 - M_{in})\dot{m}}{(1 - n_p)\rho_p} \tag{7}$$

where ρ_p is the density of the powder solid parent material.

2.3. Constitutive behaviour

Industrial conical centrifuges are typically designed so that the cone angle α is less than the angle of internal friction of the granular material, but just greater than the angle of friction for contact with the basket wall

(Swindells, 1982). Consequently the granular material slips on the internal surface of the cone rather than shearing internally. Slip is favoured by the use of smooth perforated screens with a perforation area fraction of 10-15%. The screen construction entails plates with slotted perforations or "wedge-wire sections", and the slot width is significantly less than the mean granule diameter (e.g. 75μm and 500μm, respectively, for a typical sucrose screen and sucrose crystals), see e.g. Leung (1998) or Grimwood (2005). Bizard et al. (2011) have reviewed interfacial friction laws for slurries, pastes and damp powders and propose a velocity and pressure dependent law for the shear traction τ acting on a sliding wet granular material of the form

$$\tau = au_p + bp_{eff} \tag{8}$$

where a is the slip velocity dependency coefficient, u_p the sliding velocity, b the friction coefficient and p_{eff} the interfacial effective pressure, defined as the difference between total and fluid pressures,

$$p_{eff} = p_{tot} - p_f \tag{9}$$

Note that p_{eff} is the effective normal stress acting within the solid phase or, in this particular case, between the solid phase and the screen wall, as defined by Terzaghi (1943).

Yilmazer and co-authors (Yilmazer and Kalyon, 1989; Soltani and Yilmazer, 1998) performed sliding friction experiments on densely packed suspensions of granular material within a Newtonian fluid and found the viscous slip coefficient a to be

$$a = \frac{\tilde{a}\mu_f}{d_p} \tag{10}$$

where $\tilde{a}$ is a dimensionless coefficient on the order of 25, μ_f is the interstitial fluid viscosity and d_p is the average particle size. For completeness we note that the coefficient a as given by (10) is only valid when the interface particles are completely immersed in liquid, so that this relation may not strictly apply to region III. It may be expected that a will decrease in region III due to the reduction in liquid content at the interface. We will however assume that the drain height (i.e. capillary rise height) as defined by Dombrowski and Brownell (1954) is of the same order of magnitude as the mean particle size, so that a in region III takes the same value given by (10) for regions I and II.

Since the cake of granular material slides on the surface of the cone rather than shears internally the dominant component of the radial velocity v is the sliding velocity u_p. We therefore assume that v is equal to u_p throughout the thickness of the densely packed powder. Furthermore, we will make the simplifying assumption that viscous shear in the excess fluid in Region I can be neglected so that $v(z,r) \approx u_p(r)$ for all z in all three regions, see Fig.2b.

2.4. Reference flow velocity and thickness

It is convenient to introduce a reference flow velocity u_{ref} and thickness h_{ref} in order to generate non-dimensional quantities later in the analysis. Consider the sliding flow of damp powder in Region III. The total pressure p_{tot} applied to the screen by the cake of thickness h_p and porosity n_p, under the centripetal acceleration $g^* = r\Omega^2 \sin\alpha$, is obtained from (2) as

$$p_{tot} = (1 - n_p)\, \rho_p r \Omega^2 h_p \sin\alpha \cos\alpha \quad \text{at} \quad z = 0 \tag{11}$$

A negligible quantity of fluid coats the powder, and so

$$p_{eff} = p_{tot} \tag{12}$$

The equilibrium, continuity and constitutive relationships (5-8, 6-12) can be combined to give the velocity u_{ref} at which damp (almost dry) powder slides in a spinning cone

$$u_{ref} \equiv \Omega \left(\frac{\left(1 - \hat{b}\right)(1 - n_p)\rho_p Q_p \sin\alpha}{2\pi a} \right)^{1/2} \tag{13}$$

where $\hat{b}$ is the ratio of friction coefficient to basket slope

$$\hat{b} = \frac{b}{\tan\alpha} \tag{14}$$

Note that the flow velocity is $u_p = u_{ref}$ throughout region III and is independent of r. Making use of (6,13) a reference flow thickness may be defined as

$$h_{ref} \equiv \frac{1}{r_{in}\Omega} \left(\frac{aQ_p}{2\pi\left(1 - \hat{b}\right)(1 - n_p)\,\rho_p \sin^3\alpha} \right)^{1/2} \tag{15}$$

where r_{in} is the inlet radius of the perforated basket, see Fig.3.

The associated flow thickness profile $h_p(r)$ in region III can therefore be obtained from (6) and (15) as

$$h_p = \frac{r_{in}}{r} h_{ref} \tag{16}$$

3. Design criteria

Four criteria are proposed for satisfactory operation of a conical centrifugal filter:

(1) the flow must be sufficiently thick in order for the damp particles to slide as a bulk instead of individually slipping or rolling

(2) the desaturation point must be within the cone

(3) the residual liquid content (i.e. dryness) at outlet must be satisfactory

(4) the basket structure must not fail under centrifugal loading

Note that of these criteria only (4) is an absolute design requirement. A centrifuge could be operated outside the limits defined by (1) to (3), but may then fall outside the modelling assumptions of this paper. These criteria are now presented in mathematical form.

3.1. Minimum flow thickness

In order for the centrifuge to process a large flow rate in a steady manner the flow must not be too thin, otherwise the particles will slip and roll as individual grains instead of sliding as a bulk. We term this undesirable regime *particulate flow*, in contrast with the normal *bulk flow*. We write the minimum required thickness as a multiple of the mean particle size d_p:

$$h_p \geq \tilde{d} d_p \tag{17}$$

where $\tilde{d}$ is the minimum through-thickness number of particles. In practice the value of $\tilde{d}$ required to ensure bulk flow is expected to be a function of, for example, particle shape and surface roughness. For the purpose of numerical illustrations in this paper we make the, somewhat arbitrary, choice of $\tilde{d}$=2.

Consider the case of a machine where the desaturation point is reached within the basket, so that the uppermost part of the cone is in the damp powder flow regime (region III in Fig.2). The minimum thickness is at the

outlet, see (16). Upon making use of (10) and (15-16) we can re-write the condition for bulk flow (17) in non-dimensional form as

$$\frac{h_p(r_{out})}{\tilde{d}d_p} = \frac{1}{\tilde{d}d_p\Omega l_{out}} \left(\frac{\tilde{a}\mu_f Q_p}{2\pi \left(1-\hat{b}\right)(1-n_p)\rho_p d_p \sin\alpha} \right)^{1/2} \geq 1 \qquad (18)$$

where $l_{out} = r_{out}\sin\alpha$, see Fig.3.

3.2. Desaturation position

In order to ensure that damp powder rather than a saturated paste exits the centrifuge, region III should comprise a significant fraction of the centrifuge conical basket. This is the same as requiring that region II ends well before outlet, see Fig.2. Restated, the radial coordinate at which the saturation S reaches zero $r_{S=0}$ is less than the basket size r_{out}:

$$\frac{r_{S=0} - r_{in}}{r_{out} - r_{in}} \leq \xi \qquad (19)$$

where r_{in} is the start of the perforated cone and ξ is a target dimensionless number that defines the maximum desired position of the desaturation point. For example, the choice $\xi = 1/2$ implies that the desaturation point must be in the lower half of the basket. In order to remove impurities from the crystals it is often required that a wash liquid is sprayed on the cake in regions II and III. An important requirement for efficient powder washing is the distance between the end of region II ($r = r_{S=0}$) and the lip ($r = r_{out}$). This is controlled by the choice of parameter ξ. In the sucrose industry ξ is typically 1/3, so that the top two thirds of the basket is available for powder washing.

The position of the desaturation point depends upon the relative magnitude of through-thickness drainage velocity and radial flow velocity. We

will first present some results from the literature concerning fluid drainage, and upon combining these results with an idealised model for the radial flow in the cone we will obtain an expression for the desaturation position $r_{S=0}$. For clarity the details of this idealised model for desaturation position are presented in Appendix A; only essential results are given in the main section of this work.

Centrifugal filter screens are designed in order to favour sliding (Leung, 1998) and minimize crystal losses whilst providing for minimal resistance to drainage. For simplicity we assume that the screen's resistance to fluid drainage is negligible compared to the resistance of the densely packed powder cake itself. Furthermore we assume that the cake is approximately incompressible with a constant permeability.[3]

The volumetric flow rate per unit area of fluid through a saturated powder layer q in regions I and II is obtained via Darcy's law (Darcy, 1856), as given by

$$q = \frac{k_p}{\mu_f}\left(\rho_f g^* \cos\alpha + \frac{\partial p}{\partial z}\right) \tag{20}$$

where k_p is the powder permeability, ρ_f the fluid density and $\partial p/\partial z$ the pressure gradient across the powder cake. We note that Darcy's law can be used in region II because surface tension effects are treated as negligible. The permeability k_p of a powder of mean particle size d_p and of porosity n_p has been estimated by Carman (1956) by considering Poiseuille flow of a Newtonian fluid through a bundle of capillaries. The resulting Carman-

[3]Here we assume coarse granular particles. For a compressible slurry of fine particles or flocculated/coagulated suspensions a compression rheology model may be required, see e.g. Barr and White (2006).

Kozeny equation is

$$k_p = \frac{1}{Ks^2} \frac{n_p^3}{(1-n_p)^2} \tag{21}$$

where K is a constant which depends upon the particle size distribution and shape. K has a value close to 5 for most common soils (Carman, 1956) and varies from 2 to 5.5 for sucrose crystals (Greig, 1995). s is the specific surface of the particles (the ratio of particle surface area to volume) and can be expressed in terms of the particle diameter d_p and sphericity Ψ via

$$s = \frac{6}{\Psi d_p} \tag{22}$$

For simplicity, we shall introduce an empirical parameter $\tilde{k}$ to take the particle size distribution and shape into account and re-write (21-22) as

$$k_p = \tilde{k} d_p^2 \tag{23}$$

The relation (23) is useful to make explicit the dependence of k_p upon the particle average size d_p and will be used below.

The desaturation position $r_{S=0}$ is estimated via a much simplified version of the more complete model presented in Bizard and Symons (2011), see Appendix A. Key simplifications for flow in regions I to III are listed here:

- Full sedimentation has occurred in the lower impervious cone, prior to r_{in}
- The radial velocity is equal to the basal sliding velocity through the whole thickness of the flow ($v(r,z) = u_p(r)$)
- The sliding velocity u_p in each region is taken to be constant throughout that region

- Screen resistance to drainage is negligible compared to the resistance of the densely packed powder cake

Upon making use of these assumptions we obtain (see Appendix A) the position of the desaturation point as

$$r_{S=0}^3 = r_{in}^3 + \frac{3\left(\ln\left[n_p(S_{in}-1)+1\right]+n_p\right)}{2\pi\sin^2\alpha\cos\alpha}\frac{\mu_f Q_p}{\Omega^2\rho_f k_p} \tag{24}$$

S_{in} is the saturation of the input slurry, defined as the ratio of the volume of fluid at inlet to the volume of the pores in the powder, assuming that the powder is densely packed and of porosity n_p. Thus,

$$S_{in} = \frac{(1-n_p)M_{in}\rho_p}{n_p(1-M_{in})\rho_f} \tag{25}$$

3.3. Dryness of output powder

An important feature of a centrifugal filter is how much residual liquid remains within the cake of solid particles after the majority of the liquid has been removed by drainage. Wakeman (Wakeman, 1977; Wakeman and Tarleton, 1999) has shown experimentally that the drying efficiency of a batch centrifuge is closely related to the value of a non-dimensional capillary number

$$N_{cap} = \frac{n_p^3 d_p^2 \rho_f g^*}{4\pi^2(1-n_p)^2\gamma} \tag{26}$$

where γ is the fluid surface tension and g^* is the centripetal acceleration in the basket. Wakeman gives the following experimental corellation between the ultimate relative saturation of centrifugally dried powders S_∞ and the capillary number N_{cap} as

$$S_\infty = 0.0524 N_{cap}^{-0.19} \quad \text{for} \quad 10^{-5} \leq N_{cap} \leq 0.14 \tag{27}$$

$$S_\infty = 0.0139 N_{cap}^{-0.86} \quad \text{for} \quad 0.14 \leq N_{cap} \tag{28}$$

(27-28) are plotted in Fig.4. Note that the relation between the moisture mass ratio at outlet M_{out} and the final relative saturation writes

$$S_\infty = \frac{(1-n_p)M_{out}\rho_p}{n_p(1-M_{out})\rho_f} \tag{29}$$

Wakeman's capillary number is equivalent to the more general Bond (or Eötvös) number $Bo = \rho_f g^* L^2/\gamma$ which is a measure of the importance of surface tension effects compared to body forces for a characteristic length scale L. Wakeman's results suggest that efficient centrifugal drying requires a capillary number $N_{cap} > 0.14$. For a typical powder porosity of n_p=0.4 this is equivalent to $Bo > 30$.

In the case of a conical centrifugal filter we note that drainage out of the basket is driven by the component of the centripetal acceleration normal to the screen $g^* \cos\alpha$. In addition, the moisture content of interest is that at outlet where $g^* = l_{out}\Omega^2$, see Fig.3. The relevant Bond number for a continuous centrifugal filter is thus

$$Bo = \frac{d_p^2 \rho_f l_{out} \Omega^2 \cos\alpha}{\gamma} \tag{30}$$

Industrial experience shows that for a machine of fixed size running at constant angular velocity the moisture content at outlet can be broadly independent of the flow rate, see Grimwood (2000). This suggests that the final moisture content in a continuous centrifuge may be assumed to depend only on the Bond number at outlet (with the obvious condition that the desaturation point occurs before outlet ($r_{S=0} < r_{out}$, see §3.2). We conclude that the minimum dryness condition can be written as

$$Bo \geq Bo_{dry} \tag{31}$$

where Bo_{dry} is a target dryness condition. For a particular application the value of Bo_{dry} for a required value of outlet saturation S_∞ may be determined via empirical relationships, e.g. (26-30), or by experimental measurement.

3.4. Basket failure

The maximum stress in a thin conical shell of density ρ_b, half-size at outlet l_{out} (see Fig.3) and spinning at an angular velocity Ω, is given by the hoop stress at outlet σ_ϕ:

$$\sigma_\phi = \rho_b \left(l_{out}\Omega\right)^2 \tag{32}$$

see Roark and Young (1989). Note that this calculation neglects the contribution from the small mass of the screen and its supporting mesh. Contribution to hoop stress in the shell from the mass of the flow of wet powder is also neglected. It is assumed that the basket mass is such that these additional loadings are small.

The basket will fail if the hoop stress σ_ϕ attains the yield strength σ_y. The basket integrity condition may therefore be written as

$$\sigma_\phi < \frac{\sigma_y}{\zeta} \tag{33}$$

where ζ is a safety factor which includes an allowance for the stress concentration around the drainage perforations in the basket.

4. The design domain for a continuous centrifuge

We consider the situation where a prospective user of a conical centrifugal filter wishes to obtain an estimate of the machine parameters (r_{in}, r_{out}, α, Ω, Q_p) that will satisfy the above four design criteria for a particular slurry.

The following parameters for the slurry are assumed known: (a, b, μ_f, ρ_f, ρ_p, M_{in}, n_p, d_p). As noted above, the cone angle α must be a few degrees greater than the friction angle $\arctan(b)$, see e.g. Swindells (1982) or **?**, so that the designer has the choice of (r_{in}, r_{out}, Ω, Q_p). The aim is to:

(i) determine if the technology is applicable to this application

(ii) find the optimal machine size l_{out} and speed Ω if (i) is satisfied

It will be assumed that r_{in} is small compared to r_{out} so that

$$\left(\frac{r_{in}}{r_{out}}\right)^3 \ll 1 \tag{34}$$

1) We re-write the condition for bulk flow (18) as an inequality relation between the dimensionless bulk flow parameter X_1 and the dimensionless condition C_1; according to

$$X_1(Q_p) \equiv \frac{2\pi\left(1-\hat{b}\right)(1-n_p)\,\rho_p d_p^3 \sin\alpha}{\tilde{a}\mu_f}\frac{l_{out}^2\Omega^2}{Q_p} \leq C_1 \equiv \frac{1}{\tilde{d}^2} \tag{35}$$

2) The condition for the desaturation point position (19) in the limit (34) is re-written via (23) and (24) as a relationship between the dimensionless desaturation position parameter X_2 and the dimensionless condition C_2:

$$X_2(Q_p) \equiv \frac{3\left(\ln\left[n_p(S_{in}-1)+1\right]+n_p\right)\mu_f}{2\pi\tilde{k}d_p^2\rho_f\cot\alpha}\frac{Q_p}{l_{out}^3\Omega^2} \leq C_2 \equiv \xi^3 \tag{36}$$

3) The dryness condition (31) is re-written as a relationship between the dimensionless dryness parameter X_3 and the dimensionless condition C_3:

$$X_3 \equiv \frac{1}{Bo} = \frac{\gamma}{d_p^2\rho_f\cos\alpha}\frac{1}{\Omega^2 l_{out}} \leq C_3 \equiv \frac{1}{Bo_{dry}} \tag{37}$$

4) The condition for basket failure is expressed as a relationship between the dimensionless yield parameter X_4 and the dimensionless condition C_4:

$$X_4 \equiv \frac{l_{out}\Omega}{(\sigma_y/\rho_b)^{1/2}} \leq C_4 \equiv \frac{1}{\zeta^{1/2}} \tag{38}$$

We proceed to determine a viable regime of operation $\Sigma(Q_p)$ as the (l_{out}, Ω) space in which the four conditions

$$X_i \leq C_i \text{ for } i\text{=1 to 4} \tag{39}$$

are simultaneously satisfied for any given input volumetric flow rate of powder Q_p.

5. Discussion

We now discuss the practical use of the above criteria for design of a conical centrifugal filter. We will consider the three design variables to be the basket size l_{out}, the spin velocity Ω and the input volumetric flow rate of powder Q_p. Since two criteria (X_3, X_4) are independent of Q_p but all depend upon (l_{out}, Ω) we will plot the contours of $X_i = C_i$, for $i = 1$ to 4, in the (l_{out}, Ω) plane, for selected values of Q_p.

We note that the basket outer size l_{out} and spin velocity Ω are related to the circumferential velocity v_{out} and centripetal acceleration at outlet g^*_{out} by

$$v_{out} = l_{out}\Omega \tag{40}$$

$$g^*_{out} = l_{out}\Omega^2 \tag{41}$$

respectively. Consequently, the inequalities $X_1 \leq C_1$ and $X_4 \leq C_4$ can be

written as conditions on v_{out} and $X_3 \leq C_3$ as a condition on g^*_{out} thus

$$X_1 \leq C_1 \quad \Leftrightarrow \quad v_{out} \leq v_{bulk} \equiv \left(\frac{\tilde{a}\mu_f}{2\pi \left(1-\hat{b}\right)(1-n_p)\rho_p d_p^3 \sin\alpha} \frac{Q_p}{\tilde{d}^2} \right)^{1/2} \tag{42}$$

$$X_3 \leq C_3 \quad \Leftrightarrow \quad g^*_{out} \geq g_{dry} \equiv \frac{\gamma Bo_{dry}}{d_p^2 \rho_f \cos\alpha} \tag{43}$$

$$X_4 \leq C_4 \quad \Leftrightarrow \quad v_{out} \leq v_{bkf} \equiv \left(\frac{\sigma_y}{\zeta \rho_b} \right)^{1/2} \tag{44}$$

where v_{bulk} and v_{bkf} are the limiting circumferential velocities for the bulk flow and basket failure conditions respectively. g_{dry} is the minimum centripetal acceleration at outlet to achieve the required dryness.

The condition on desaturation point position X_2 (36) depends upon a combination of both v_{out} and g^*_{out} and, consequently, cannot be expressed in such a simple form as that of (42-44). Note that both the criterion (42) for bulk flow X_1 and criterion (44) for basket failure X_4 each implies a maximum circumferential velocity. One of these two criteria will be the more restrictive, depending upon the particular flow rate Q_p considered.

In order to discuss the practical use of the above results we will make use of the typical case of sucrose-molasses separation, with the numerical values given in Tables 1, 2 and 3.

5.1. Viable regime of operation $\Sigma(Q_p)$

The possible design area $\Sigma(Q_p)$ may be plotted in the (l_{out}, Ω) plane as follows. Criteria X_3 and X_4 (dryness and basket failure) are independent of flow rate Q_p and are plotted first to define an initial triangular regime, marked as the combined white and dark grey wedges in Fig.5. The addition of the

flow rate dependent criteria X_1 and X_2 (bulk flow and desaturation point) for a particular choice of flow rate Q_p further restricts the viable operating regime. This area is plotted in dark grey in Fig.5 for the typical case of Q_p = 3 m^3 s^{-1}. In this particular case criterion X_4 is the dominant constraint for v_{out}, and X_1 is redundant.

The four design criteria result in a triangular zone of operation Σ, the corners of which are labeled a, b, c in Fig.5.

5.2. Effect of flow rate upon the operating regime

The input flow rate of powder Q_p influences the bulk flow (X_1) and desaturation point (X_2) criteria, see (35), (36). This is demonstrated in Fig.6a for the case of sucrose massecuite with the values given in Tables 1-3: two flow rates ($Q_p = 8 \times 10^{-7}$ m^3/s and $Q_p = 4 \times 10^{-4}$ m^3/s) are assumed. Design domains for a greater number of values of Q_p are plotted in Fig.6b. A number of features appear in Fig.6b:

- there exists a range of values of Q_p for which Σ is not empty, between a minimum flow rate Q_p^{min} and a maximum flow rate Q_p^{max}. At either of these two limit flow rates the design domain Σ reduces to a single point in the (l_{out}, Ω) plane
- when the flow rate is increased progressively from Q_p^{min} to Q_p^{max} the design zone first expands until it reaches a maximum size for a particular flow rate Q_p^{opt}, and then shrinks down until Q_p reaches Q_p^{max}
- there is a minimum basket size l_{out}^{min}, defined by the intersection of the $X_1 = C_1$ and $X_2 = C_2$ contours.

These features are detailed below.

5.2.1. Maximum and minimum flow rates

As shown in Fig.6b the maximum flow rate Q_p^{max} and the corresponding size l_{out}^{max} are obtained when the desaturation point X_2 (36), dryness X_3 (37) and basket failure X_4 (38) conditions are all satisfied. Solving (36), (37), (38) simultaneously for (Q_p, l_{out}) yields

$$Q_p^{max} \equiv \frac{2\pi\tilde{k}}{3Bo_{dry}} \frac{\cos\alpha}{\tan\alpha} \frac{\xi^3}{(\ln\left[n_p(S_{in}-1)+1\right]+n_p)} \frac{d_p^4\rho_f^2}{\gamma\mu_f} \left(\frac{\sigma_y}{\zeta\rho_b}\right)^2 \tag{45}$$

$$l_{out}^{max} \equiv \frac{\cos\alpha}{Bo_{dry}} \frac{d_p^2\rho_f}{\gamma} \frac{\sigma_y}{\zeta\rho_b} \tag{46}$$

In similar fashion the minimum flow rate Q_p^{min} and the corresponding size l_{out}^{min} is reached when the bulk flow X_1 (35), desaturation point X_2 (36) and dryness X_3 (37) conditions are all attained. Solving (35), (36), (37) simultaneously for (Q_p, l_{out}) yields

$$Q_p^{min} \equiv \frac{6\pi Bo_{dry}\tilde{d}^4}{\tilde{a}^2\tilde{k}} \frac{\sin^3\alpha}{\cos^2\alpha}(1-\hat{b})^2(1-n_p)^3 \frac{(\ln\left[n_p(S_{in}-1)+1\right]+n_p)}{\xi^3}\overline{\rho}^2\frac{\gamma d_p^2}{\mu_f} \tag{47}$$

$$l_{out}^{min} \equiv \frac{3\tilde{d}^2}{\tilde{a}\tilde{k}} \frac{\sin^2\alpha}{\cos\alpha}(1-\hat{b})(1-n_p) \frac{(\ln\left[n_p(S_{in}-1)+1\right]+n_p)}{\xi^3}\overline{\rho}d_p \tag{48}$$

$$\tag{49}$$

For $Q_p = Q_p^{min}$ the circumferential velocity at outlet is a minimum:

$$v_{out}^{min} \equiv \left(\frac{3Bo_{dry}\tilde{d}^2}{\tilde{a}\tilde{k}} \tan^2\alpha(1-\hat{b})(1-n_p) \frac{(\ln\left[n_p(S_{in}-1)+1\right]+n_p)}{\xi^3}\overline{\rho}\frac{\gamma}{d_p\mu_f}\right)^{1/2} \tag{50}$$

For the numerical values given in Tables 1 - 3 we obtain $Q_p^{min} = 8\times10^{-8}\mathrm{m}^3/\mathrm{s}$ and $Q_p^{max} = 0.52\mathrm{m}^3/\mathrm{s}$.

5.2.2. The particular value of flow rate Q_p^{opt}

Intermediate between Q_p^{min} and Q_p^{max} is a value of Q_p that gives the largest viable operating regime $\Sigma(Q_p)$. This flow rate Q_p^{opt} may be considered optimal in the sense that it allows the design criteria to be met with the widest possible range of machine sizes l_{out} and operating speeds Ω. The value Q_p^{opt} is obtained for the particular case where the two limits on the circumferential velocity X_1 (42) and X_4 (44) are simultaneously attained (see Fig.6b). Upon solving this system of two equations we obtain

$$Q_p^{opt} \equiv \frac{2\pi\tilde{d}^2}{\tilde{a}} \sin\alpha \left(1-\hat{b}\right)(1-n_p)\frac{\rho_p d_p^3}{\mu_f}\frac{\sigma_y}{\zeta\rho_b} \tag{51}$$

We note that the choice $Q_p = Q_p^{opt}$ allows for the largest possible centripetal acceleration at outlet, obtained from (36) and (51) as

$$g_{out}^{max} \equiv \frac{\tilde{a}\tilde{k}}{3\tilde{d}^2}\frac{\cot\alpha}{\sin\alpha}\frac{1}{(1-\hat{b})(1-n_p)}\frac{\xi^3}{(\ln\left[n_p(S_{in}-1)+1\right]+n_p)}\frac{1}{d_p\overline{\rho}}\frac{\sigma_y}{\zeta\rho_b} \tag{52}$$

for the design point

$$l_{out} = l_{out}^{min} \tag{53}$$

$$\text{and} \quad \Omega = \Omega^{max} \equiv \frac{\tilde{a}\tilde{k}\xi^3\cot\alpha\csc\alpha}{3(1-\hat{b})d_p\tilde{d}^2\left(\ln\left[n_p(S_{in}-1)+1\right]+n_p\right)(1-n_p)\overline{\rho}}\left(\frac{\sigma_y}{\zeta\rho_b}\right)^{1/2} \tag{54}$$

For the numerical values given in Tables 1-3 we obtain $Q_p^{opt} = 2.0\times10^{-4}\mathrm{m}^3/\mathrm{s}$, $g_{out}^{max} = 1.3\times10^7\mathrm{m/s}^2$, $\Omega^{max} = 7.9\times10^4\mathrm{rad\ s}^{-1}$.

5.3. Viable design domain, independent of Q_p

As shown in Fig.6b there exists a domain outside of which a conical centrifugal filter would not work for any input flow rate Q_p. The boundaries

of this domain are simply given by

$$v_{out} \leq v_{bkf} \tag{55}$$

$$g^*_{out} \geq g_{dry} \tag{56}$$

$$l_{out} \geq l^{min}_{out} \tag{57}$$

For simplicity the coordinates of the corners of the envelope design surface are not detailed here but can be easily obtained from (40-41) and (55-57). The viable design domain for sucrose massecuite and a duplex steel basket is shown in Fig.7.

5.4. Feasibility of a conical continuous centrifugal filter

If the condition

$$Q^{min}_p \leq Q^{max}_p \tag{58}$$

is not satisfied for a choice of powder, liquid and basket material there exists no operating point (l_{out}, Ω, Q_p) that would make a conical centrifuge work. Upon combining (45), (47), (58) we obtain the following condition for existence of a viable design

$$\frac{3Bo_{dry}\tilde{d}^2}{\tilde{a}\tilde{k}} \tan^2\alpha(1-\hat{b})(1-n_p)\frac{(\ln\left[n_p(S_{in}-1)+1\right]+n_p)}{\xi^3}\overline{\rho}\frac{\gamma}{d_p\rho_f}\frac{\zeta\rho_b}{\sigma_y} \leq 1 \tag{59}$$

Note that (59) is independent of (l_{out}, Ω, Q_p) and is a function only of the slurry and basket properties.

6. Conclusion

Design criteria for conical centrifugal filters are written explicitly as functions of the basket size l_{out}, spinning velocity Ω and input flow rate of powder

Q_p. Regions of potential operating points (l_{out}, Ω) are given for a wide range of values of Q_p and analytical expressions are given for minimum and maximum values of these three parameters as functions of the slurry and basket properties. A condition is obtained for feasibility of a conical centrifugal filter depending on the slurry and basket properties.

7. Acknowledgements

The authors are grateful to the Ashby Scholarship Fund for financial support.

Appendix A - Desaturation position: a simple model

The desaturation position is estimated via a simplified version of a more complete model for a desaturating granular flow in a spinning perforated cone presented in Bizard and Symons (2011). The key simplifying assumptions used here are that: 1) there is a constant sliding velocity in each region (I to III), and 2) the screen provides negligible resistance to drainage. These idealisations allow the fluid conservation problem to be reduced to differential equations with constant coefficients, and thus allow analytical expressions to be obtained for the desaturation point position.

We will make use of the same non-dimensionalization procedure adopted in Bizard and Symons (2011) to obtain the dimensionless parameters as

$$H_f = \frac{h_f}{h_{ref}} \quad ; \quad H_p = \frac{h_p}{h_{ref}} \quad ; \quad R = \frac{r}{r_{in}} \quad ; \quad U_p = \frac{u_p}{u_{ref}} \quad ; \quad \overline{\rho} = \frac{\rho_p}{\rho_f} \quad (60)$$

where h_f and h_p are the powder and fluid thicknesses, see Fig.8. The reference velocity u_{ref} and thickness h_{ref} are defined in (13) and (15).

The aim is to obtain the radial coordinate at which region II ends: $R_{S=0}$. In the case of slender flow the downstream conditions do not affect the upstream flow Bizard et al. (2011), so that in order to obtain $R_{S=0}$ we only need to model regions I and II. For each of these two regions we will first calculate the sliding velocity U_p using the simplifying assumption that the cake is of constant liquid content: the saturation S is taken as 1 in region I and 0.5 in region II (see Fig.8). Evolution of the fluid layer thickness H_f is then obtained by considering fluid conservation in the basket.

7.1. Sliding velocity

Radial equilibrium of the cake is obtained from (5-8)

$$au_p + bp_{eff} = p_{tot} \tan \alpha \tag{61}$$

where the total pressure applied by the cake on the interface p_{tot} reads

$$p_{tot} = ((1 - n_p)\rho_p + n_p S \rho_f)\, r\Omega^2 h_p \cos\alpha \sin\alpha \tag{62}$$

The effective pressure at the interface is the difference between the total pressure p_{tot} and the fluid pressure p_f. However, as we neglect the resistance to flow of the screen p_f vanishes at the interface $z = 0$ and we obtain $p_{eff} = p_{tot}$ (12). Uniform porosity n_p and a constant input mass flow rate of solid $(1 - M_{in})\dot{m}$ dictates that the powder volumetric flow rate Q_p (6) is conserved throughout the cone (powder losses through the screen are neglected).

In most practical cases the input slurry is just above saturation ($S_{in} \gtrapprox 1$). In order to obtain the sliding velocity U_p^I and cake thickness profile $H_p^I(R)$ in region I we will consider a cake of constant saturation $S = 1$, see Fig.8a: the mass of excess fluid is neglected. Note that this model is thus not valid for

input slurries for which $S_{in} \gg 1$. In region II the flow evolves from saturated powder ($S = 1$) at $R = R_{S=1}$ to damp powder ($S \approx 0$) at $R = R_{S=0}$. In order to obtain the velocity U_p^{II} and thickness $H_p^{II}(R)$ in region II we will thus consider a half-saturated cake ($S = 0.5$), see Fig.8a.

Upon making use of (60) we obtain the dimensionless thickness and velocity profiles from (6, 12 and 61) as

$$H_p = \left(\frac{(1 - n_p)\, \rho_p}{(1 - n_p)\rho_p + n_p S \rho_f} \right)^{1/2} \frac{1}{R} \tag{63}$$

$$U_p = \left(\frac{(1 - n_p)\rho_p + n_p S \rho_f}{(1 - n_p)\, \rho_p} \right)^{1/2} \tag{64}$$

where it is assumed that S = 1, 0.5 and 0 in regions I, II and III respectively.

7.2. Fluid conservation

7.2.1. Region I

For fluid volume conservation in region I we assume that the entire thickness of slurry slides at a constant speed u_p^I with a layer of densely packed saturated powder of thickness h_p^I and a top layer of pure fluid of thickness $(h_f^I - h_p^I)$, see Fig.8b. Recall that we have assumed that full sedimentation has already occurred in the lower impervious cone.

Consider volume conservation in the circular element of radial width dr and perimeter $2\pi r \sin\alpha$ located at a radial coordinate r shown in Fig.9. Seepage in the radial direction is assumed negligible and the volumetric flow rate of liquid entering this element is therefore

$$Q_{conv}^I(r) = 2\pi r \sin\alpha \left(h_f^I - (1 - n_p) h_p^I \right) u_p^I \tag{65}$$

The volumetric flow rate of liquid seeping out of the same element and

through the screen is calculated from Darcy's law (20) as

$$dQ^I_{seep} = \frac{2\pi k_p r g^* \rho_f h^I_f \sin\alpha\cos\alpha}{\mu_f h^I_p} dr \tag{66}$$

Upon making use of (65-66), we obtain the fluid mass conservation relation for the element shown in Fig.9 as a non-linear ordinary differential equation (ODE) in r:

$$\frac{d}{dr}[Q^I_{conv}] + \frac{dQ^I_{seep}}{dr} = 0 \tag{67}$$

The associated initial condition is given by the flow rate of fluid at inlet:

$$\rho_f Q^I_{conv} = M_{in}\dot{m} \quad \text{at} \quad r = r_{in} \tag{68}$$

We re-write the ODE (67) in a non-dimensional form via (60, 63-66)

$$\frac{dH^I_f}{dR} = -\left(\frac{1}{R} + ZR^2\right) H^I_f \tag{69}$$

where the dimensionless group Z Bizard and Symons (2011) reads

$$Z \equiv \frac{k_p \rho_f \Omega^2 r^2_{in} \sin\alpha\cos\alpha}{\mu_f h_{ref} u_{ref}} \equiv \frac{2\pi\Omega^2 \rho_f k_p r^3_{in} \sin^2\alpha\cos\alpha}{\mu_f Q_p} \tag{70}$$

Z is the ratio of the through-thickness flow rate of interstitial fluid via drainage to the radial flow rate of powder.

The initial condition (68) is also re-written in a non-dimensional form via (60, 63-65)

$$H^I_f(1) = [n_p(S_{in} - 1) + 1] H^I_p(1) \tag{71}$$

Solving (69) for $H^I_f(R)$ yields the fluid thickness profile in region I as

$$H^I_f(R) = \frac{H^I_f(1)}{R} e^{\frac{Z}{3}\left(1 - R^3\right)} \tag{72}$$

Region I ends when the liquid level reaches the powder level and therefore the saturation S=1, i.e. when $H_f^I(R) = H_p^I(R)$. $R_{S=1}$ can be obtained from (71-72) as

$$R_{S=1} \equiv \frac{r_{S=1}}{r_{in}} = \left(1 + \frac{3}{Z}\ln[n_p(S_{in} - 1) + 1]\right)^{1/3} \tag{73}$$

7.2.2. Region II

Consider volume conservation in the circular element of radial width dr and perimeter $2\pi r \sin\alpha$ located at a radial coordinate r shown in Fig.10.

The liquid flow rate out of the element of width dr at the coordinate r shown in Fig.10 is

$$dQ_{seep}^{II} = \frac{2\pi\rho_f k_p r g^* \cos\alpha \sin\alpha}{\mu_f} dr \tag{74}$$

and transport of fluid via the radial displacement of densely packed powder leads to the following convective volumetric flow rate:

$$Q_{conv}^{II}(r) = 2\pi n_p r h_f^{II} u_p^{II} \sin\alpha \tag{75}$$

Fluid conservation in the element of the saturated layer shown in Fig.10 then yields the ODE

$$\frac{d}{dr}[Q_{conv}^{II}] + \frac{dQ_{seep}^{II}}{dr} = 0 \tag{76}$$

We express the fluid conservation equation (76) in a dimensionless form via (60), (74-75)

$$\frac{dH_f^{II}}{dR} = -\frac{RZ}{n_p U_p^{II}} - \frac{H_f^{II}(R)}{R} \tag{77}$$

and upon taking the initial condition for region II as

$$H_f^{II}(R_{S=1}) = H_p^{II}(R_{S=1}) \tag{78}$$

we obtain the fluid thickness profile in region II

$$H_f^{II}(R) = \frac{1}{n_p U_p^{II} R}\left((\ln[n_p(S_{in}-1)+1]+n_p) + \frac{Z}{3}(1-R^3)\right) \tag{79}$$

The radial coordinate at which the fluid thickness vanishes $R_{S=0}$ is obtained from (79)

$$R_{S=0} \equiv \frac{r_{S=0}}{r_{in}} = \left(1 + \frac{3}{Z}\left(\ln[n_p(S_{in}-1)+1]+n_p\right)\right)^{1/3} \tag{80}$$

7.3. Accuracy of simplified model

This simplified model introduces a discontinuity in velocity (and therefore also cake thickness) at $R = R_{S=1}$ and $R = R_{S=0}$ due to the discontinuity in saturation S assumed to obtain the flow velocity (64). However, numerical results show that its prediction for the value of $R_{S=0}$ is close to that of the more complete model developed in Bizard and Symons (2011) for a typical sucrose machine (Tables 1-3). In Fig.11 the fluid and cake thickness profiles given by the simplified model are plotted (thick lines) together with the results of the complete model (thin lines). Because the simple model does not allow any internal shear of the flow it overestimates the initial fluid and cake thicknesses. On the other hand the simple model also neglects any resistance of the screen to drainage and the fluid level H_f descends more steeply. These two simplifications therefore almost offset each other in terms of prediction of the desaturation point location.

Values of $R_{S=0}$ predicted by the simple model presented in this paper and the more complete model of Bizard and Symons (2011) are compared in Fig.12. Contours of $R_{S=0}$ are plotted for a range of values of seepage number Z, screen permeability κ and relative density $\overline{\rho}$ (for constant M_{in} and n_p and

hence varying S_{in}, see (25)). κ is the ratio of the screen permeability to the densely packed powder as defined by Bizard and Symons (2011). When κ exceeds 10^{-1} the value of $R_{S=0}$ lies close to that predicted by the complete model of Bizard and Symons (2011) over a wide range of Z and $\overline{\rho}$.

References

Barr, J.D. and White, L.R. (2006), 'Centrifugal drum filtration: I. A compression rheology model of cake formation', *American Institute of Chemical Engineers Journal* . **52**(2), 545–556.

Bizard, A. F. M., Symons, D. D., Fleck, N. A. and Durban, D. (2011), 'Flow of damp powder in a rotating impervious cone', *Journal of Applied Mechanics* **78**, 021017-1-10.

Bizard, A.F.M. and Symons, D.D. (2011), 'Flow of wet powder in a conical centrifugal filter - an analytical model', *Chemical Engineering Science* . **66**, 6014–6027.

Bruin, S. (1969), 'Velocity distributions in a liquid film flowing over a rotating conical surface', *Chemical Engineering Science* **24**(11), 1647–1654.

Carman, P. C. (1956), *Flow of Gases through Porous Media*, (Butterworths Scientific Publications, London, UK)

Darcy, H. (1856), 'Determination des lois d'ecoulement de l'eau à travers le sable', *Les Fontaines Publiques de la Ville de Dijon* .

Dombrowski, H.S. and Brownell, L.E. (1954), 'Residual equilibrium saturation of porous media', *Industrial and Engineering Chemistry* **46**(6), 1207–1219.

Greig, C. (1995), 'Phd thesis: Studies on continuous sugar centrifuges', *Department of chemical engineering, University of Queensland* .

Grimwood, C. (2000), 'Chapter 14 - Centrifugation' *in Handbook of Sugar Refining, Chi Chou, C. (ed)*, (Wiley, New York, USA), pp 203–244

Grimwood, C. (2005), 'Chapter 7 - Filtering centrifuges' *in Solid/Liquid Separation - Scale-up of Industrial Equipment, Wakeman, R.J. and Tarleton, S. (eds)*, (Elsevier, UK). pp 314–374

Grimwood, G. and Ferrier, C. (1972), 'Discharge of solid particles from centrifugal machine', *United States Patent and Trademark Office* (04/876229).

Leung, W. W.-F. (1998), *Industrial centrifugation technology*, McGraw-Hill, New York.

Makarytchev, S. V., Langrish, T. A. G. and Prince, R. G. H. (1998), 'Structure and regimes of liquid film flow in spinning cone columns', *Chemical Engineering Science* **53**(8), 1541–1550.

Makarytchev, S. V., Xue, E., Langrish, T. A. G. and Prince, R. G. H. (1997), 'On modelling fluid flow over a rotating conical surface', *Chemical Engineering Science* **52**(6), 1055–1057.

Norbury, R.J. and White, E.T. (1973), Preliminary studies on the breakage

of sugar crystals on impact, *Proc. of the 40th Conference of the Queensland Society of Sugar Cane Technologists*, 171–179.

Roark, R. J. and Young, W. C. (1989), *Roark's formulas for stress and strain*, 6th edn, McGraw-Hill, New York.

Soltani, F. and Yilmazer, U. (1998), 'Slip velocity and slip layer thickness in flow of concentrated suspensions', *Journal of Applied Polymer Science* **70**(3), 515–522.

Swindells, R. (1982), 'Phd thesis: A mathematical model of a continuous sugar centrifuge', *Department of chemical engineering, University of Queensland* .

Swindells, R. J. and White, E. T. (1980), 'Breakage of sugar crystals on impact', *Sugar Journal* **43**(2), 23–25.

Symons, D. D. (2011*a*), 'Frictional flow of damp granular material in a conical centrifuge', *Proc. IMechE Part C: J. of Mechanical Engineering Science.* **226**, 1055–1057.

Symons, D. D. (2011*b*), 'Integral methods for flow in a conical centrifuge', *Chemical Engineering Science* **66**(13), 94–103.

Terzaghi, K. (1943), *Theoretical soil mechanics*, J. Wiley and Sons. New York.

Yilmazer, U. and Kalyon, D.M. (1989), 'Slip effects in capillary and parallel disk torsional flows of highly filled suspensions', *Journal of Rheology* **33**, 1197–1212.

Wakeman, R. (1977), 'Dewatering properties of particulate beds', *Journal of Powder and Bulk Solids Technology* pp. 64–69.

Wakeman, R. J. and Tarleton, E. S. (1999), *Filtration : Equipment selection, modelling and process simulation*, Elsevier Science Ltd.

[Figure 1 about here.]

[Figure 2 about here.]

[Figure 3 about here.]

[Figure 4 about here.]

[Figure 5 about here.]

[Figure 6 about here.]

[Figure 7 about here.]

[Figure 8 about here.]

[Figure 9 about here.]

[Figure 10 about here.]

[Figure 11 about here.]

[Figure 12 about here.]

[Table 1 about here.]

[Table 2 about here.]

[Table 3 about here.]

List of Figures

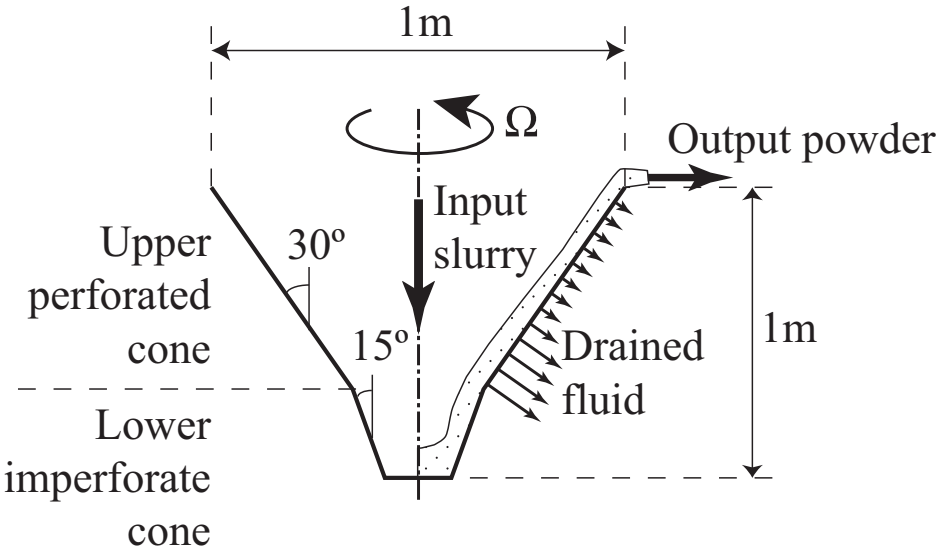

Figure 1: Section of a typical continuous centrifugal filter

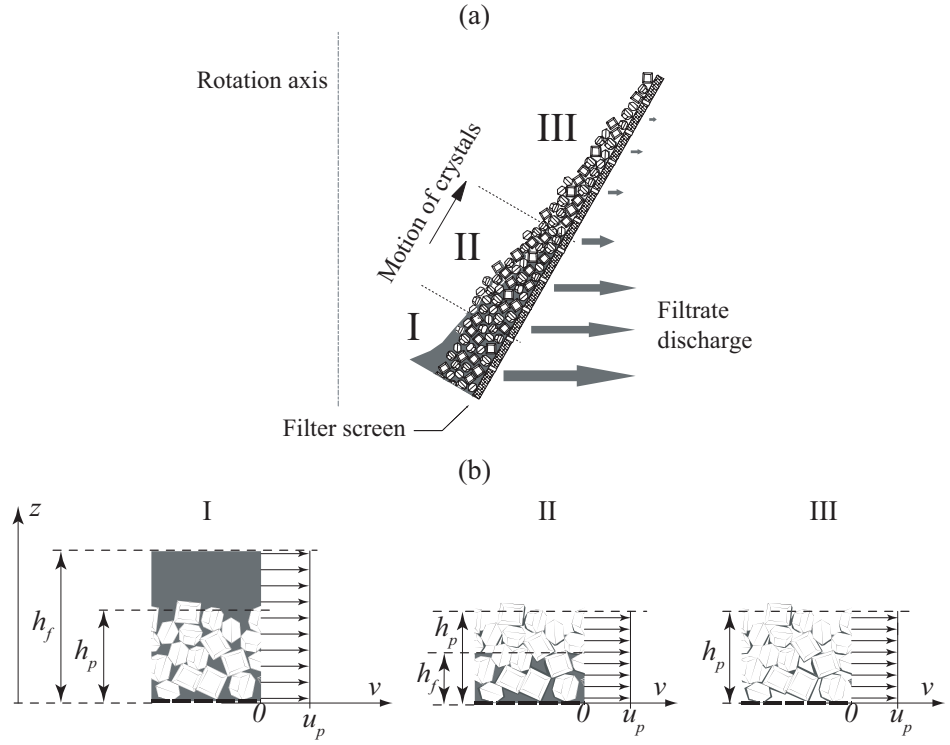

Figure 2: (a) Flow in a rotating perforated cone and (b) microstructure and velocity profile of the solid/liquid/air phases in regions I, II and III for the simple situation where all powder has sedimented before inlet

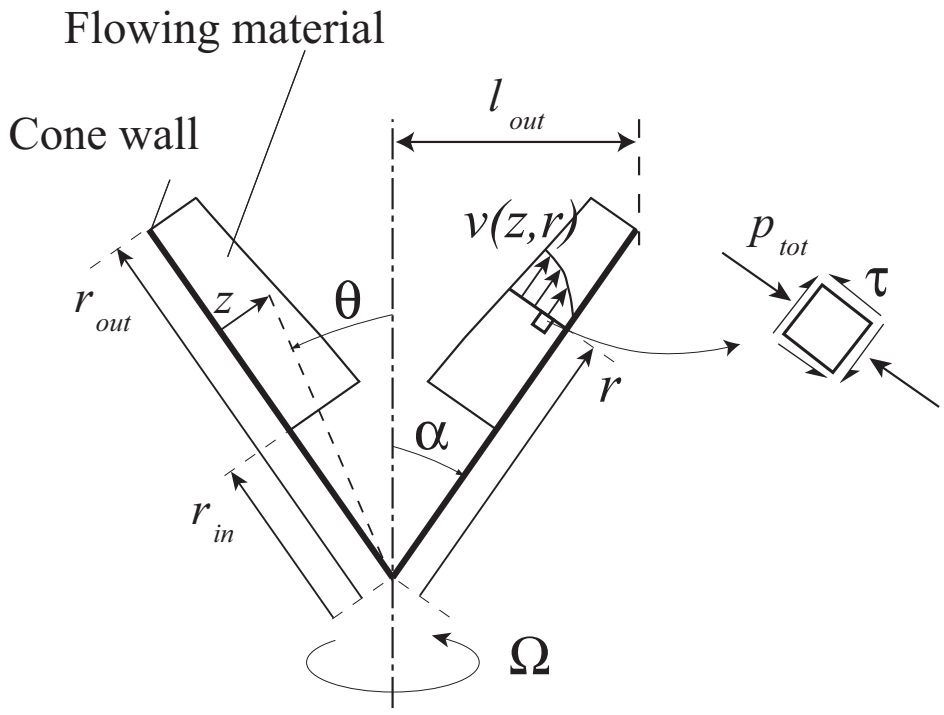

Figure 3: Model geometry

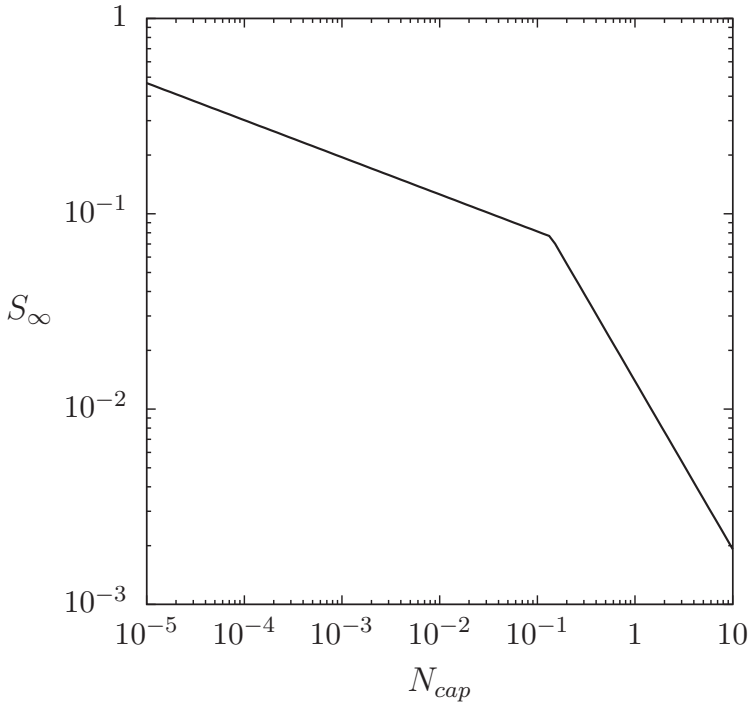

Figure 4: Residual saturation against capillary number (from Wakeman (1977))

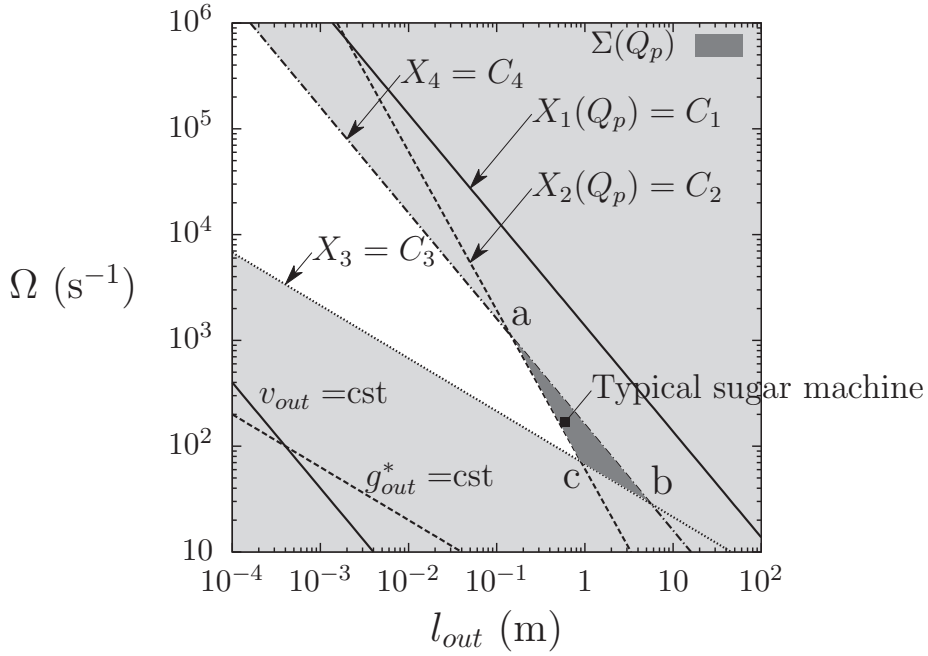

Figure 5: Range of possible basket sizes and spinning velocities for sucrose massecuite with an input powder volumeteric flow rate $Q_p = 2.9 \times 10^{-3}\mathrm{m}^3/\mathrm{s}$

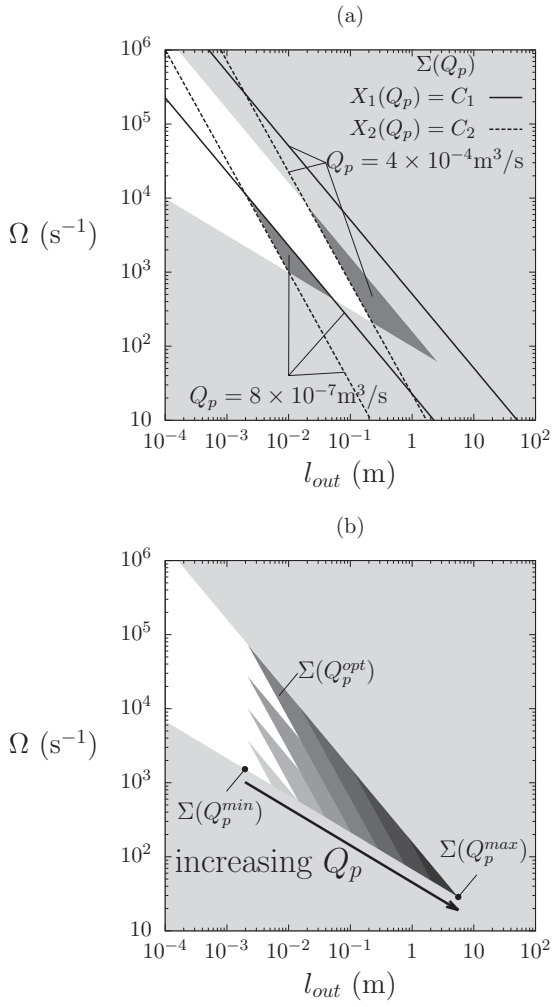

Figure 6: Sucrose massecuite: (a) Construction of the design zone Σ for two different values of Q_p (b) Evolution of Σ as Q_p increases

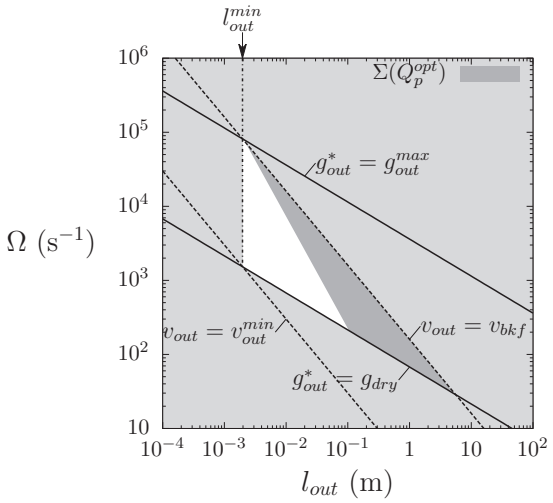

Figure 7: Sucrose massecuite: Envelope design domain, independent of Q_p

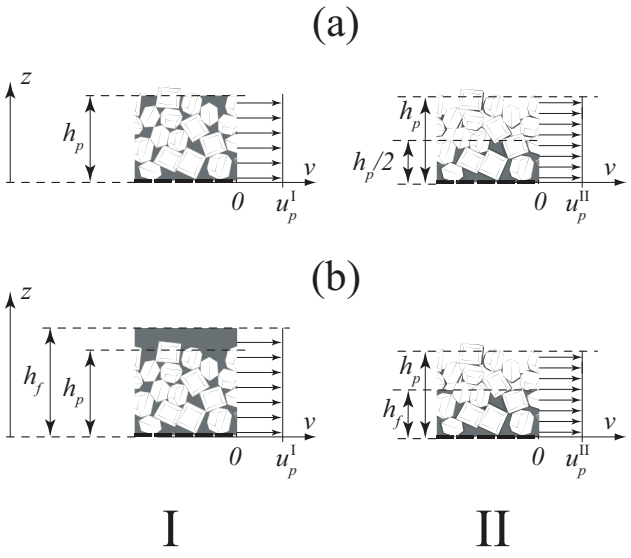

Figure 8: Microstructure considered in regions I and II for (a) equilibrium and (b) fluid conservation

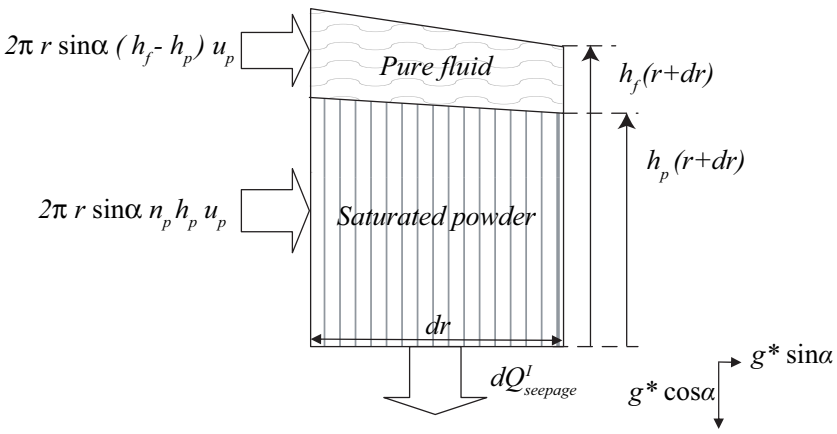

Figure 9: Region I: Volume fluxes of fluid through a control volume of width $2\pi r \sin\alpha$ and length dr subjected to a local gravity of amplitude $g^* = r\Omega^2 \sin\alpha$

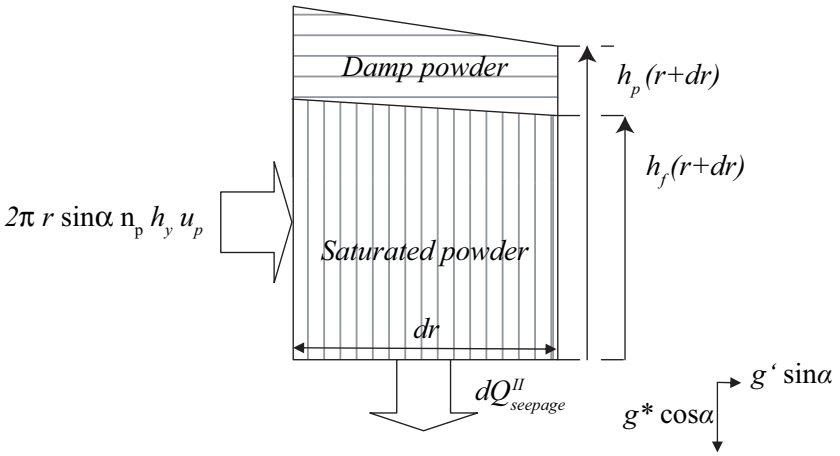

Figure 10: Region II: Volume fluxes of fluid through a control volume of width $2\pi r \sin\alpha$ and length dr subjected to a local gravity of amplitude $g^* = r\Omega^2 \sin\alpha$

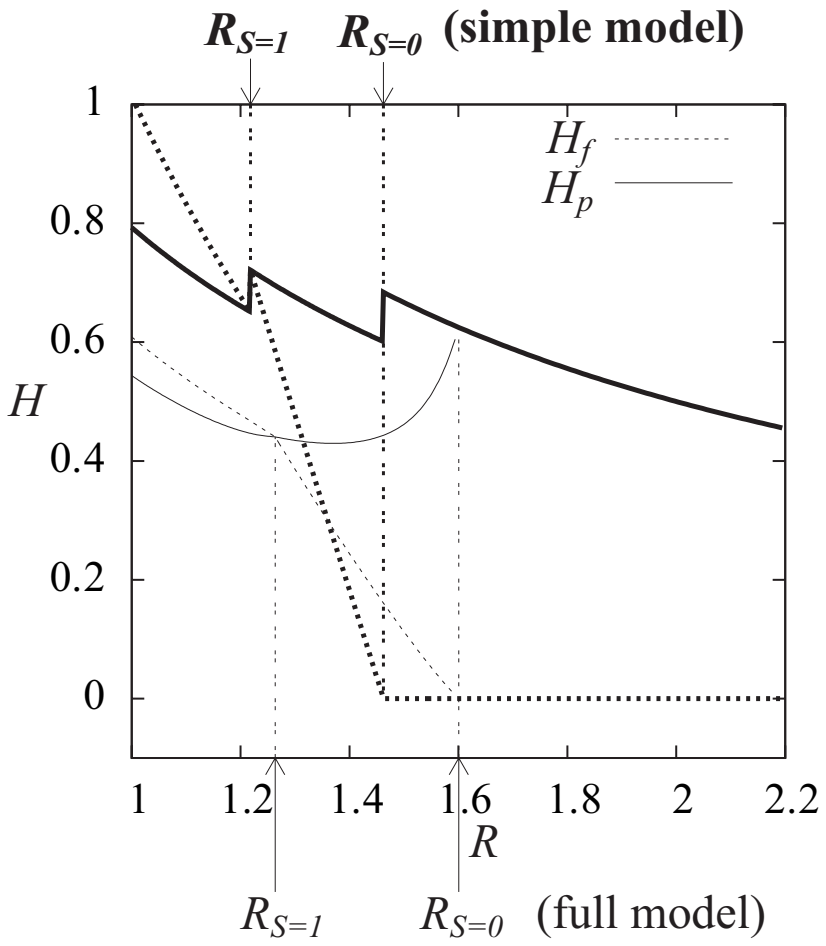

Figure 11: Comparison between the thickness profiles predicted by the complete flow model (thin lines) and the simplified model (thick lines) for typical values of a sucrose centrifuge

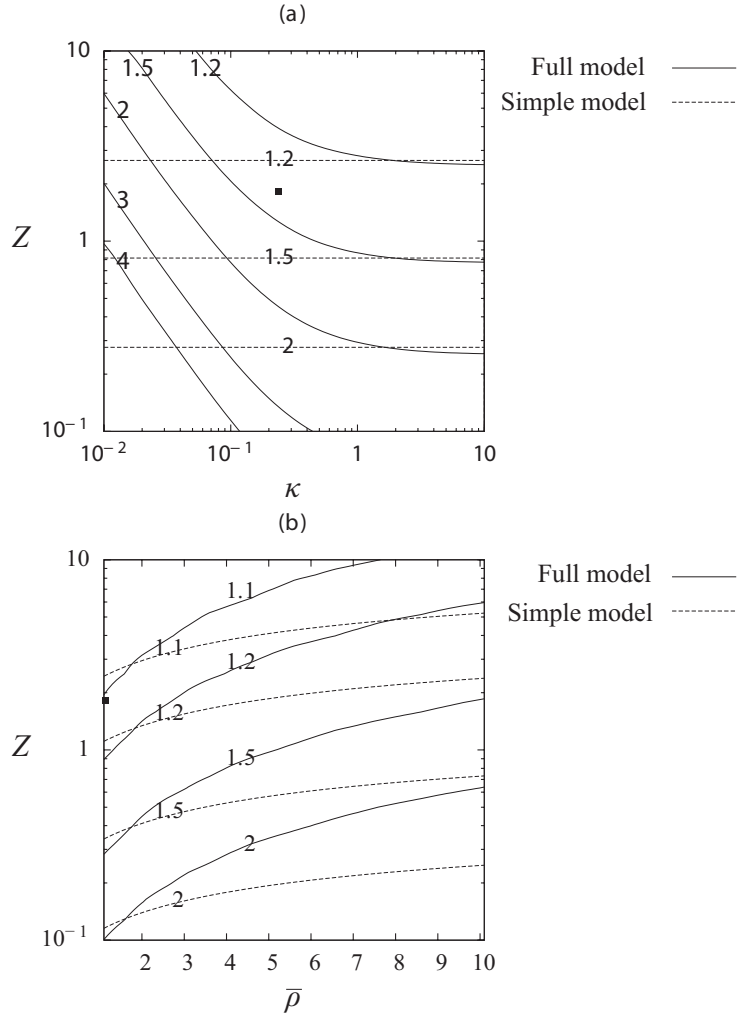

Figure 12: Comparison between the position of the desaturation point predicted by the complete flow model (solid lines) and the simplified model (dashed lines) for typical values of a sucrose centrifuge. The working point of the typical sucrose centrifuge considered earlier is marked with a black square

List of Tables

Cone

r_{in} (m)	r_{out} (m)	Ω (rad s^{-1})	α (°)	ρ_b (kg m^{-3})	σ_y (MPa)
0.54	1.185	188.5	30	7800	600

Input slurry

$\dot{m}$ (kg s^{-1})	M_{in} (%)
5.6	50

Powder

ρ_p (kg m^{-3})	d_p (μm)	n_p (%)	b	k_p (m^2)
1580	500	40	0.5	5×10^{-10}

Fluid

ρ_f (kg m^{-3})	μ_f (Pa s)	γ (mN m^{-1})
1400	1	50

Table 1: Parameters considered for a typical sucrose centrifuge

R_{out}	$\hat{b}$	Z	κ	$\overline{\rho}$	$Ro(r_{out})$	$Bo(r_{out})$
2.2	0.87	1.8	0.18	1.1	0.0013	128

Table 2: Dimensionless parameters for the typical sucrose centrifuge described in Table 1

$\tilde{d}$	ξ	Bo_{dry}	ζ
2	1	30	3
$C_1 \equiv \tilde{d}^{-2}$	$C_2 \equiv \xi^3$	$C_3 \equiv Bo_{dry}^{-1}$	$C_4 \equiv \zeta^{-1/2}$
0.25	1	0.033	0.58

Table 3: Design targets for a typical sucrose centrifuge